Structure
Article

Structural Basis for DNA Recognition by FoxO1 and Its Regulation by Posttranslational Modification

Michael M. Brent,[1,2] Ruchi Anand,[1] and Ronen Marmorstein[1,2,*]
[1]The Wistar Institute
[2]The Department of Chemistry
University of Pennsylvania, Philadelphia, PA 19104, USA
*Correspondence: marmor@wistar.org
DOI 10.1016/j.str.2008.06.013

SUMMARY

FoxO transcription factors regulate the transcription of genes that control metabolism, cellular proliferation, stress tolerance, and possibly life span. A number of posttranslational modifications within the forkhead DNA-binding domain regulate FoxO-mediated transcription. We describe the crystal structures of FoxO1 bound to three different DNA elements and measure the change in FoxO1-DNA affinity with acetylation and phosphorylation. The structures reveal additional contacts and increased DNA distortion for the highest affinity DNA site. The flexible wing 2 region of the forkhead domain was not observed in the structures but is necessary for DNA binding, and we show that p300 acetylation in wing 2 reduces DNA affinity. We also show that MST1 phosphorylation of FoxO1 prevents high-affinity DNA binding. The observation that FoxO-DNA affinity varies between response elements and with posttranslational modifications suggests that modulation of FoxO-DNA affinity is an important component of FoxO regulation in health and misregulation in disease.

INTRODUCTION

FoxO1 belongs to a family of transcription factors that share a conserved 100 amino acid forkhead box, or winged helix, DNA-binding domain (DBD). The nomenclature for the more than 100 members of this gene family has been standardized such that all members start with Fox (Forkhead box), followed by a letter to distinguish 17 subfamilies, and a number to distinguish individual members (Kaestner et al., 2000) (Figure 1). The many members of this family are emerging as critical regulators of development, immunity, metabolism, and cancer. The FoxO subfamily has been shown to play roles in apoptosis, stress resistance, cell cycle arrest, DNA damage repair response, and glucose metabolism in mammalian cells (Greer and Brunet, 2005). In addition, recent mouse knockout studies have shown that FoxOs are tumor suppressors (Paik et al., 2007). FoxO also represents the closest human homologs of the *Caenorhabditis elegans* longevity gene *daf-16*, the downstream target of *daf-2* insulin/IGF-I receptor, and *C. elegans sir-2.1* (Kenyon et al., 1993; Mazet et al., 2003; Tissenbaum and Guarente, 2001). In humans, FoxO activity is regulated by a number of posttranslational modifications (Huang and Tindall, 2007) (Figure 1), and misregulation of FoxO has been shown to play a role in diseases of aging (Anderson et al., 1998; Borkhardt et al., 1997; Cheong et al., 2003; Davis et al., 1994; Galili et al., 1993; Hillion et al., 1997; Hu et al., 2004; Modur et al., 2002; Parry et al., 1994; Seoane et al., 2004; Sunters et al., 2006).

Previous structures of the FoxA3/HNF-3γ, FoxD3/Genesis, FoxP2, and FoxK1a/ILF-1 forkhead domains bound to their DNA consensus sequences have revealed a compact three-helix fold, with the third helix sitting in the major groove of B-form DNA, and C-terminal β strands projecting along the axis of the DNA to contact one or both of the adjacent minor grooves (Clark et al., 1993; Jin et al., 1999; Stroud et al., 2006; Tsai et al., 2006). Solution structures have also been reported for FoxO4/AFX and FoxC2/FREAC11 (van Dongen et al., 2000; Weigelt et al., 2001). The FoxA3/HNF-3γ structure, the namesake of the winged helix domain, was the first reported, and it revealed two well-ordered loops, or wings, contacting each of the adjacent minor grooves (Clark et al., 1993). Later structures revealed significant diversity in DNA binding, particularly in the C-terminal wing 2 region. The FoxD3/Genesis, FoxK1a/ILF-1, and FoxP2 structures all contain a combination of α helix and loop in the wing 2 region and mediate divergent interactions with DNA (Jin et al., 1999; Liu et al., 2002; Stroud et al., 2006; Tsai et al., 2006). Outside of the conserved DNA-binding motif, forkhead transcription factors also show important differences in their domain structure, expression, regulation, and disease association (Myatt and Lam, 2007).

FoxO1 was originally named FKHR, or forkhead in rhabdomyosarcomas, because of its association with a chromosomal translocation in alveolar rhabdomyosarcoma (Galili et al., 1993). Later, *daf-16*, the *C. elegans* homolog of FoxO1/FKHR, was characterized as a key downstream target in the insulin/IGF-1 signaling pathway that is required for mutations in the insulin/IGF-1-like receptor *daf-2* to confer increased life span in a *C. elegans* longevity model (Gottlieb and Ruvkun, 1994; Kenyon et al., 1993; Larsen et al., 1995; Ogg et al., 1997). This pathway is well conserved in humans, where nutrient abundance triggers insulin/IGF-1 receptor signaling that leads to Akt phosphorylation of FoxO1 at Thr24, Ser256, and Ser319 (Brunet et al., 1999; Rena et al., 1999; Tang et al., 1999). This phosphorylation causes an interaction with 14-3-3 proteins that localizes FoxO1 to the cytoplasm to block transcriptional activation by FoxO1 (Brunet et al., 1999). Both CDK1 and CDK2 have been reported to phosphorylate FoxO1 at Ser249, to regulate subcellular localization of FoxO1 (Huang et al., 2006; Yuan et al., 2008). The effect of this modification on

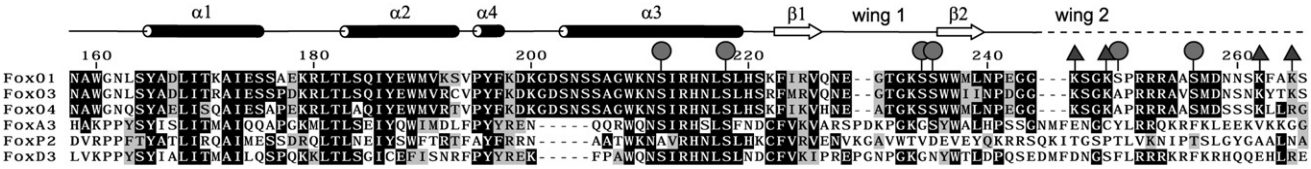

Figure 1. FoxO1 Secondary Structure and Sequence Alignment of Human FoxO1 DBD with Other Forkhead Domains
Residues that undergo phosphorylation or acetylation are marked with a circle or a triangle respectively.

FoxO1 localization and activity is controversial, with CDK1 reported to cause nuclear localization and transcriptional activation (Yuan et al., 2008), and CDK2 reported to cause cytoplasmic localization and inhibition of FoxO1 (Huang et al., 2006). MST1 kinase has been shown to phosphorylate four sites on FoxO3, Ser207, Ser213, Ser229, and Ser230, in response to oxidative stress in neurons (Lehtinen et al., 2006). This phosphorylation is reported to disrupt FoxO's interaction with 14-3-3 proteins and to allow nuclear translocation of FoxO, where it initiates apoptotic cell death (Lehtinen et al., 2006). The MST1 sites are conserved in FoxO1 and are also likely targets of MST1 regulation.

In addition to phosphorylation, the DBD of FoxO can be acetylated by CBP/p300, and FoxO can be deacetylated by SIRT1 and SIRT2, which are human homologs of the yeast Sir2 longevity protein (Brunet et al., 2004; Fukuoka et al., 2003; Jing et al., 2007; Motta et al., 2004; van der Horst et al., 2004). This provides an additional level of control over the FoxO transcription factors and a connection to the Sir2 model for longevity by calorie restriction. It has been shown that acetylation of three lysines, all within or near the DBD of FoxO1, reduces the affinity of FoxO1 for target DNA and increases Akt phosphorylation of FoxO1 (Jing et al., 2007; Matsuzaki et al., 2005). The biological effects of the acetylation state of FoxO are diverse and dependent on both the family member (FoxO1, FoxO3, FoxO4, and FoxO6) and the cellular context. Deacetylation of FoxO3 by SIRT1 is associated with repressed FoxO-induced apoptosis (Motta et al., 2004); however, in response to oxidative stress, SIRT1 deacetylation of FoxO3 promotes cell cycle arrest and resistance to oxidative stress (Brunet et al., 2004). In adipocytes, SIRT2 deacetylation of FoxO1 causes FoxO1 to suppress adipogenesis through its transcriptional regulation of cell cycle inhibitors (Jing et al., 2007; Nakae et al., 2003).

The posttranslational modifications discussed here only represent the phosphorylation and acetylation sites within or near the DBD of FoxO1, or amino acids 158–248 in the case of FoxO1. These sites are interesting from a structural perspective because they may regulate FoxO1 activity in different ways. They may disrupt or enhance DNA binding directly or they may mediate protein-protein interactions that regulate FoxO1. Yet another factor that is reported to be important for regulation of target gene expression by forkhead transcription factors is variations in affinity for different DNA response elements. For FoxA transcription factor in *C. elegans*, it is reported that high-affinity DNA elements cause FoxA target genes to be expressed earlier in embryonic development and low-affinity DNA elements cause delayed onset of target gene expression (Gaudet and Mango, 2002).

Here, we report structures of the FoxO1 DBD bound to closely related recognition elements: the insulin response element (IRE) with the consensus sequence of TT(G/A)TTT**TG** was the first recognition element reported for FoxO1 (Brunet et al., 1999; Guo et al., 1999; Kops et al., 1999; Tang et al., 1999) and the Daf-16 family binding element (DBE) with the consensus sequence of TT(G/A)TTT**AC**, which is bound by FoxO1 more strongly (Furuyama et al., 2000). We also report a third structure of FoxO1 DBD bound to a higher affinity DBE sequence, called DBE2 here, which reveals that FoxO1 bending of the flanking bases outside of the eight-base consensus sequence may be important for optimal DNA binding by FoxO1. We then measure the effect of acetylation and phosphorylation on DNA binding affinity of FoxO1 to provide a structural basis for DNA recognition and posttranslational regulation of FoxO1.

RESULTS

Structures of FoxO1 DBD Bound to DBE and IRE DNA

Structures of the FoxO1 DBD bound to 16-base-pair DNA containing the DBE recognition sequence of 5′-TTGTTTAC-3′ or the IRE recognition sequence of 5′-TTGTTTTG-3′ were determined to 2.1 Å and 2.2 Å, respectively (Table 1 and Figure 2). The structures reveal the expected forkhead, or winged helix, DNA-binding motif with helix 3 binding in the major groove of the DNA and the side chains of Asn211 and His215 making all of the direct base-specific contacts (Figures 2B and 2C; Figure 3). Side chains of Asn158 and Tyr165 from the N terminus of the DBD and Arg225, Ser234, Ser235, and Trp237 from wing 1 make phosphate contacts to adjacent minor grooves of the DNA (Figure 3). The 2.9 Å structure of FoxO1 bound to the high-affinity DBE2 DNA sequence shows the same interactions around helix 3; however, it also shows a greater amount of bend in the six base pairs flanking the DBE consensus sequence, where wing 2 is predicted to make interactions (Figure 2D). Interestingly, unlike previously reported forkhead structures, electron density was not observed for the C-terminal wing 2 region of the FoxO1 DBD, suggesting that it is flexible and disordered in the crystals. Given the lack of sequence homology to other forkhead subfamilies in this region (Figure 1) and the previously observed structural diversity at the C terminus of forkhead domains, this finding was not surprising but required further investigation as described below.

Wing 2 Is Flexible but Essential for DNA Binding

The extent of FoxO1 DBD wing 2 interactions with DNA was not known at the start of this study. By sequence alignment, wing 2 was predicted to start at Lys245 and possibly extend as far as Ser256, the target of Akt phosphorylation. To be inclusive of all posttranslational modification sites, we crystallized and determined the structure of FoxO1 151–266 bound to the IRE and DBE2 sequences, but electron density was not observed for residues 242–266. To rule out proteolysis during crystal preparation, FoxO1/IRE crystals were redissolved in water, and TOF mass

Table 1. Data Collection and Refinement Statistics for FoxO1/DNA Complexes

	FoxO1/IRE DNA			FoxO1/DBE1 DNA	FoxO1/DBE2 DNA
	Native	Hg S184C	Hg A207C	Native	Native
Data Collection					
Wavelength (Å)	0.88560	1.54178	1.54178	1.00000	0.97949
Space Group	$P2_12_12$	I222	I222	I222	$P3_2$
a, b, c (Å)	76.06	65.40	65.30	65.52	99.64
	102.43	76.17	76.66	76.44	99.64
	65.45	102.34	102.36	102.14	98.47
α, β, γ (°)	90, 90, 90	90, 90, 90	90, 90, 90	90, 90, 90	90, 90, 120
Resolution (Å)	30–2.2	30–3.1	30–3.2	30–2.1	30–2.9
Redundancy	11.0 (9.9)	5.1 (5.0)	6.2 (5.8)	4.8 (4.9)	4.3 (4.3)
Completeness (%)	99.4 (98.1)	99.3 (98.9)	99.8 (99.5)	99.9 (100.0)	99.6 (99.8)
R_{sym} (%)	6.4 (32.7)	11.8 (31.1)	16.0 (37.3)	7.2 (34.0)	8.8 (32.4)
I/σ (I)	39.4 (6.9)	12.8 (6.9)	11.9 (6.3)	20.2 (4.5)	15.7 (4.9)
Phasing Analysis					
Resolution (Å)	30–3.20				
Number of sites	2				
Figure of merit (FOM)	0.40				
Refinement					
Resolution (Å)	30–2.21			30–2.10	30–2.91
Number of reflections	26167			15307	23754
R_{work}/R_{free}	21.5/24.9			21.1/25.5	26.7/27.6
B factors (Å^2)					
All atoms	30.1			39.9	69.0
Protein	26.0			35.9	69.1
DNA	34.1			43.2	68.9
Water	31.7			44.3	54.1
Ions	53.1			60.5	N/A
Ramachandran plot					
Most favored	94.9%			92.6%	80.4%
Allowed	5.1%			4.9%	19.6%
Generously allowed	0.0%			2.5%	0.0%
Disallowed	0.0%			0.0%	0.0%
Rms deviations					
Bond lengths (Å)	0.008			0.008	0.007
Bond angles (°)	1.3			1.3	1.2

Data sets were collected from a single crystal. Values in parentheses are for the highest resolution shell. R_{free} was calculated using 10% of the reflection data chosen randomly and omitted at the start of refinement.

spectrometry was performed to confirm the presence of full-length protein in the crystals (see Figure S1A available online). We then mapped the extent of wing 2 contributions to DNA binding by preparing four FoxO1 DBD constructs with varying wing 2 lengths and measuring DNA binding using electrophoretic mobility shift assay (EMSA) (Figures 4A–D). FoxO1 constructs 151–266 and 151–256 both bound to the IRE and DBE2 sequences with roughly equal affinity. FoxO1 151–249 also bound to the DBE2 sequence with roughly equal affinity, whereas binding of the IRE sequence was reduced by several fold. Surprisingly, the FoxO1 151–244 construct showed no detectable binding to IRE or DBE2 DNA, indicating that some or all of wing 2 residues 244–249 are required for FoxO1 to bind DNA. To rule out an artifact of the EMSA, we also performed the same assay on 151–244 by fluorescence polarization using 151–266 as a positive control, and we observed the same result (Figure S1B).

These findings suggest that amino acids 244–249 are flexible but nonetheless important for DNA binding, most likely through phosphate contacts by Lys245 and Lys248. Previous reports have suggested that the wing 2 region of FoxO may be more flexible than the rest of the protein. Specifically, wing 2 was found to be disordered in a FoxO4 DBD solution structure (without DNA) by NMR (Weigelt et al., 2001). Molecular Dynamics simulations of a theoretical FoxO/DNA complex also suggested that wing 2 may be more flexible than the rest of the DBD (Boura et al., 2007).

To lend further support to the hypothesis that wing 2 is the most flexible part of the FoxO1 DBD even in the presence of DNA, we performed limited proteolysis of FoxO1 151–266 in the

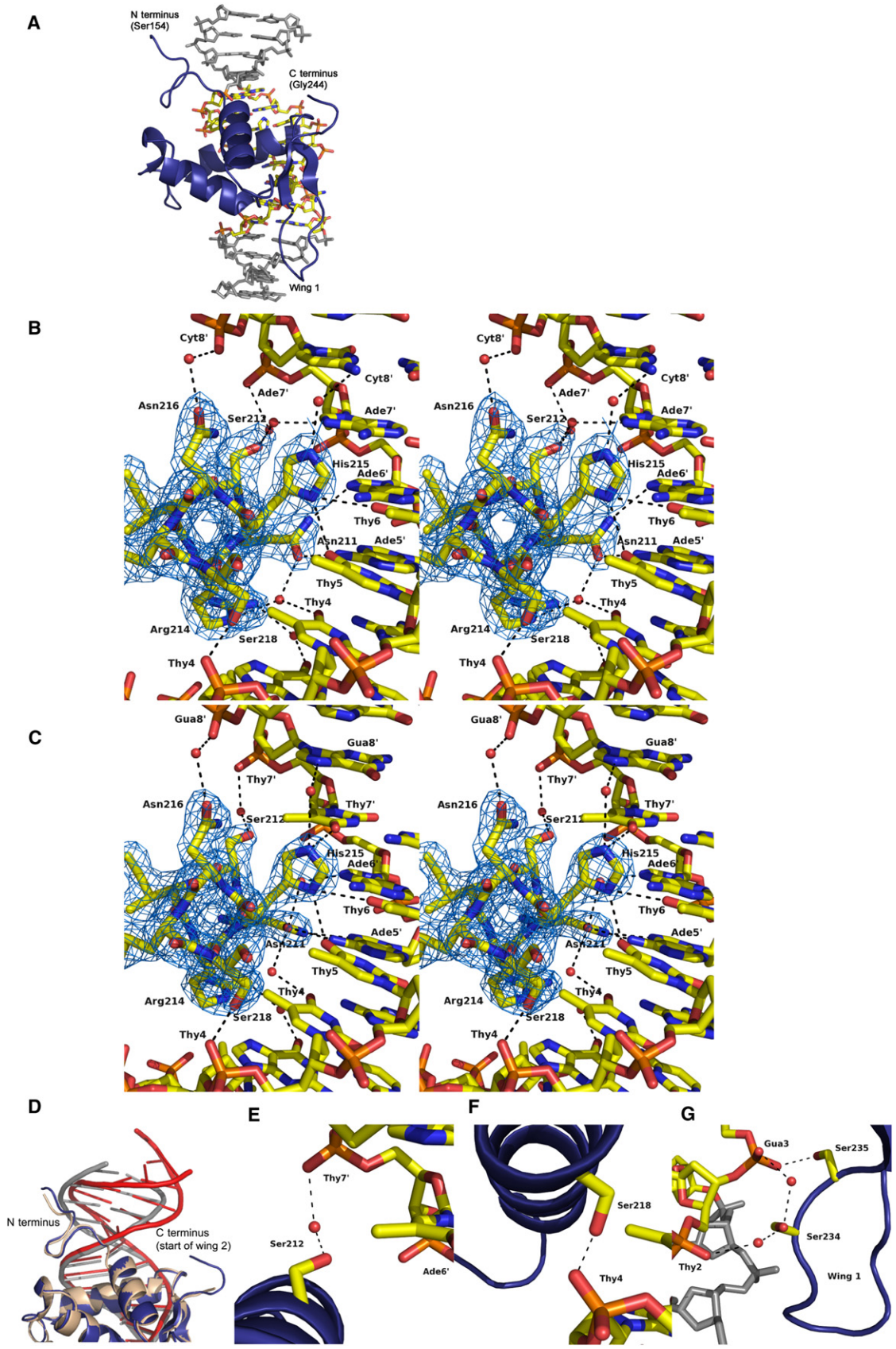
A
N terminus
(Ser154)
C terminus
(Gly244)
Wing 1
B
Cyt8'
Ade7'
Asn216
Ser212
His215
Ade6'
Thy6
Asn211
Ade5'
Thy5
Thy4
Arg214
Ser218
C
Gua8'
Thy7'
D
N terminus
C terminus
(start of wing 2)
E
F
G
Gua3
Ser235
Ser234
Thy2
Wing 1

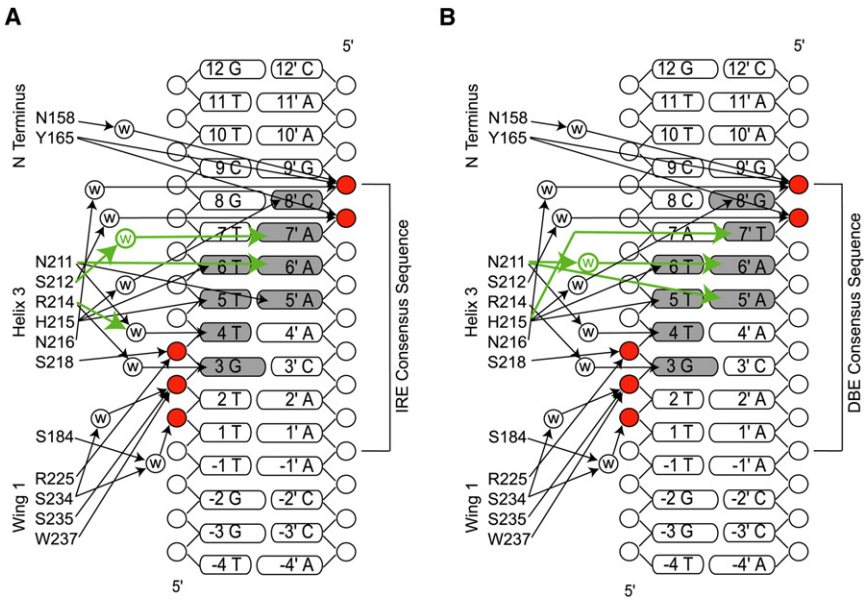

Figure 3. Schematic Showing FoxO1 DBD Interactions with IRE and DBE1 DNA Sequences

(A and B) Differences in hydrogen bonding between the DBE and IRE sequences are highlighted in green. Bases that are contacted directly or through water-mediated interactions are shaded. Phosphates that are contacted directly or through water-mediated interactions are highlighted in red.

presence of a 3-fold excess of DBE2 DNA and sequenced the proteolysis products by N-terminal Edman degradation (Figure S2A–E). The results confirmed that papain, proteinase K, and trypsin all remove C-terminal amino acids preferentially, even in the presence of DNA. Trypsin also removed N-terminal amino acids 151–157. TOF mass spectrometry of the papain digestion product confirmed that papain removes amino acids 245–266, but the remaining FoxO1 151–244 is stable toward papain. These results indicate that residues 245–266 are flexible and accessible to protease digestion, even in the presence of a 3-fold molar excess DBE2 DNA. These data, and the observation that the S249E mutation does not affect DNA-binding by Fox01 (see CDK phosphorylation), indicate a minimal FoxO1 DBD of residues 158–248 and a short but essential wing 2 comprising residues 245–248. There also seems to be some DNA binding contribution from arginines 250–252 under certain circumstances.

Structural Basis for High-Affinity Binding of DBE Sequences

When the bases flanking the FoxO consensus sequence are kept the same, the FoxO1 DBD binds to the DBE1 DNA with 2-fold greater affinity, compared with the IRE DNA (Figure 5A). High-resolution structures reveal that the DBE and IRE consensus sequences are bound with different hydrogen-bonding and water-mediated interactions through the versatile side chains of Asn211 and His215 (Figures 2B and 2C; Figure 3). The overall structural differences between the two FoxO1/DNA complexes are quite small, with an alignment rmsd of less than 0.2 Å. However, the network of hydrogen bonds is different at the protein/DNA interface as a result of the different arrangement of hydrogen bond donors and acceptors in the major groove of the DNA around bases 7′ and 8′.

In the FoxO1/DBE structure, Asn211 forms bidentate hydrogen bonds with Ade5′ (Figure 2C). His215 in the FoxO1/DBE structure is protonated with delocalized positive charge between ND1 and NE2 mediating direct interactions with Thy7′, Thy5, and Thy6, which are within 3.07, 2.90, and 3.07 Å, respectively, and forming a water-mediated hydrogen bond to N7 of Gua8′. In the FoxO1/IRE structure, the Asn211 side chain is oriented parallel with the DNA axis (Figure 2B) and is hydrogen bonding with Ade5′ and Ade6′. His215 in the FoxO1/IRE structure is still interacting with Thy5 and Thy6, and makes a water-mediated hydrogen bond to Cyt8′ in place of Gua8′ of the DBE sequence; however, Ade7′, replacing Thy7′ of the DBE sequence, lacks a hydrogen bond acceptor for His215. Instead, the hydrogen bond–donating amino group of Ade7′ is 3.47 Å away from His215 and is unlikely to be contributing to protein-DNA affinity. We believe that this difference at base 7′ accounts for the modest 2-fold increased affinity of FoxO1 for the DBE1 sequence versus the IRE sequence (Figure 5A).

The DBE2 DNA sequence contains the same 8-base consensus sequence as DBE1 DNA, but the 3′ flanking sequence is two bases longer and has been replaced with the 5′-ATTTTG-3′ sequence. The 5′-NTTT-3′ sequence is a high-affinity consensus sequence for the 3′ flanking region enriched by random oligonucleotide selection using mouse FoxO1 DBD, which shares an identical sequence to human FoxO1 within the DBD (Furuyama et al., 2000). An analysis of 1387 putative human DBE sequences in the Database of Transcriptional Start Sites (http://dbtss.hgc.jp) suggests that thymine-rich 3′ flanking sequences are also present in the human genome. We observed a 5-fold increase in affinity of FoxO1 DBD for DBE2 DNA versus DBE1 DNA (Figure 5A). The structure of the FoxO1 DBD/DBE2 DNA complex exhibits the same binding motif as the DBE1 structure, but in contrast to

Figure 2. Structures of FoxO1/DNA Complexes

(A) Representative FoxO1 DBD/DNA complex: 2.1 Å structure of FoxO1 bound to the DBE1 sequence. The eight base DBE sequence is in CPK coloring, and flanking bases are gray.

(B and C) Stereo view of helix 3 interactions with DNA showing the different interactions with IRE (panel b) and DBE (panel c) DNA-mediated by Asn211 and His215. Electron density shown is from a simulated annealing omit map contoured at 1.0 σ around the DNA recognition helix.

(D) Superposition of FoxO1 DBD bound to DBE1 and DBE2 DNAs to illustrate the larger amount of bend in the DNA for the DBE2 structure. FoxO1 DBD bound to DBE1 is colored in blue and gray. FoxO1 DBD bound to DBE2 is colored in tan and red.

(E–G) The targets of MST1 phosphorylation and their interactions with the phosphate backbone of DNA. Structure shown is FoxO1 DBD/DBE1 DNA. The interactions are conserved in the FoxO1/IRE DNA structure: panel e, Ser212; panel f, Ser218; and panel g, Ser234 and Ser235.

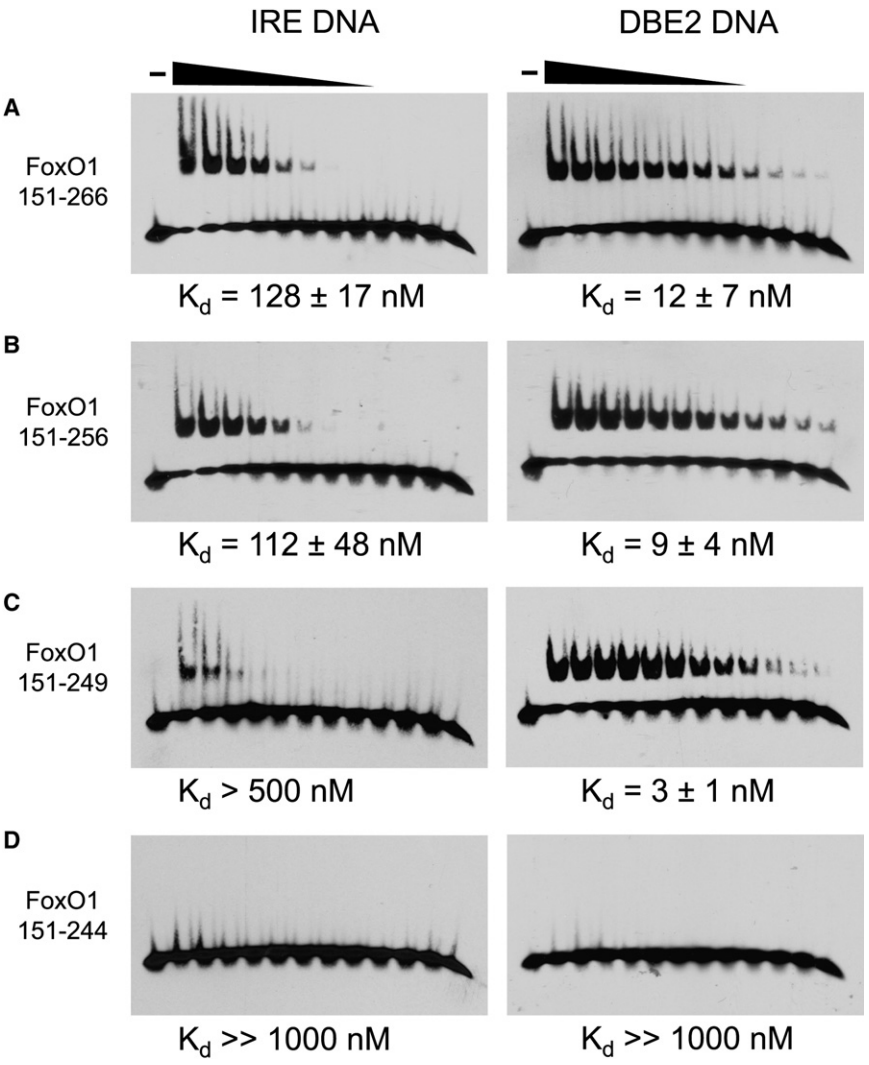

Figure 4. Binding of FoxO1 DBD and Truncation Mutants to Cognate DNA Sites
(A–D) EMSA binding studies to IRE and DBE2 DNA using C-terminally truncated FoxO1 DBD constructs.

the DBE1 structure, the DBE2 structure reveals bent and distorted DNA in the 3′ flanking region, where wing 2 of FoxO1 is predicted to make interactions with the DNA minor groove (Figure 2D).

MST1 Phosphorylation Blocks DNA Binding

MST1 kinase is reported to phosphorylate four serines within the forkhead domains of FoxO1 and FoxO3 to promote FoxO translocation to the nucleus and expression of cell death target genes (Lehtinen et al., 2006). The FoxO1/DNA structures reported here, however, reveal that these four serines (Ser212, Ser218, Ser234, and Ser235) all make either direct or water-mediated hydrogen bond interactions with the phosphate backbone of the DNA (Figure 2E–G). On the basis of this observation, we hypothesized that MST1 phosphorylated FoxO1 would be unable to bind DNA as a result of steric and electrostatic repulsion of the negatively charged phosphoserines and the negatively charged DNA backbone. To directly measure the effect of MST1 phosphorylation on DNA affinity, we phosphorylated the FoxO1 DBD with MST1 and purified the reaction product by gel filtration. TOF mass spectrometry confirmed the addition of four phosphates (Figure S3A). EMSA was done on the MST1 phosphorylated sample and an unmodified control to measure affinity for the DBE2 and IRE sequences (Figure 5B). The assay reveals that MST1-phosphorylated FoxO1 shows almost no detectable binding to either DBE2 or IRE DNA for the 1 μM to 0.5 nM FoxO1 concentration range tested. To rule out an artifact of the EMSA, we also measured affinity for DBE2 DNA by fluorescence polarization using MST1 phosphorylated FoxO1 and unmodified FoxO1 as a positive control, and we observed the same result (Figure S3C). This finding is not necessarily inconsistent with the observation that MST1 activates FoxO; however, it suggests that there are additional steps, probably involving phosphatase activity, in the pathway for MST1 activation of FoxO.

CBP/p300 Acetylation Reduces DNA Binding

Previous studies have investigated the in vivo effect of FoxO acetylation on DNA binding (Daitoku et al., 2004). In vitro DNA-binding assays have also been done in which CBP/p300 target lysines are mutated to alanine, glutamine, or arginine (Matsuzaki et al., 2005). These studies show that removal of the positive charge at Lys245, 248, and 262 reduces DNA binding and transcription of FoxO target genes. To more directly measure the effect of CBP/p300 acetylation on DNA affinity in vitro, we acetylated the FoxO1 DBD with p300 and purified the reaction product by gel filtration. We used a combination of proteolysis and TOF mass spectrometry to confirm that four acetyl groups were added to lysines 245, 248, 262, and 265 (Figure S2B; Figure S4A–C). The fourth acetyl group at Lys265 was not previously reported but is consistent with preference of CBP/p300 for acetylating KXXK sequences. EMSA was performed on the p300 acetylated sample and an unmodified control to measure affinity for the DBE2 and IRE sequences (Figure 5C). The assay reveals that the DNA-binding affinity of p300 acetylated FoxO1 is reduced by approximately three fold to the DBE2 sequence and close to two fold to the IRE sequence. These results reveal that CBP/p300 acetylation of the FoxO1 DBD does indeed cause a modest reduction in DNA binding in vitro.

DNA Binding Is Unchanged by Akt or CDK Phosphorylation

The sites of Akt and CDK1/2 phosphorylation (serines 256 and 249, respectively) are reported to regulate FoxO1 through

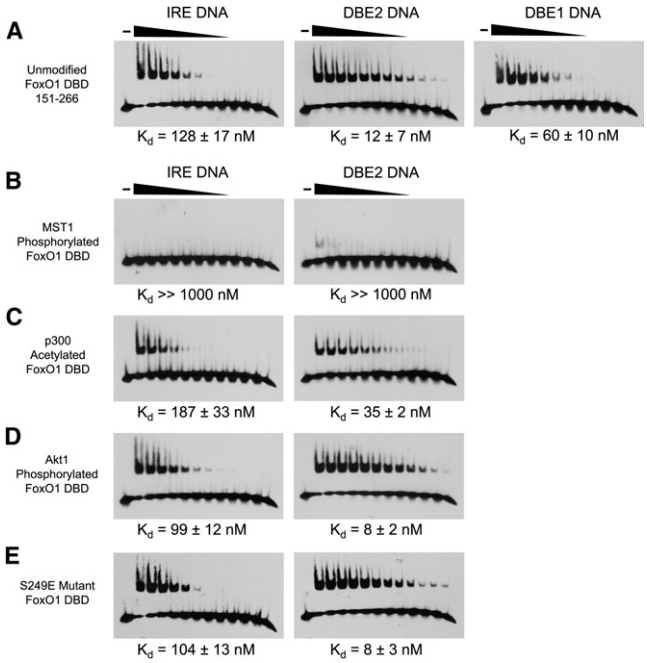

Figure 5. Binding of Unmodified and Posttranslationally Modified FoxO1 DBD to Cognate DNA Sites

(A) EMSA binding studies showing the difference in affinity for FoxO1 151-266 binding to IRE, DBE2 and DBE1 DNA sequences.

(B–E) EMSA results showing the effects of specified FoxO1 151-266 modifications on binding affinity for IRE and DBE2 DNA sequences.

mechanisms unrelated to DNA binding. Phosphorylation of Ser256 by Akt has been shown to regulate FoxO1 by causing an inhibitory interaction with 14-3-3 proteins. Phosphorylation of Ser249 is proposed to either disrupt the FoxO1/14-3-3 interaction in the cytoplasm or interfere with the adjacent nuclear localization signal (NLS, arginines 251–253).To test the possibility that phosphorylation of these two sites may also reduce FoxO1 activity by interfering with DNA binding, we used Akt kinase to phosphorylate Ser256, and we prepared a S249E mutant to mimic CDK phosphorylated FoxO1. For the Akt phosphorylated sample, TOF mass spectrometry was done to confirm the addition of one phosphate (Figure S5). CDK2 was inactive toward the FoxO1 DBD because of the absence of the C-terminal regions of FoxO1, amino acids 267–655, as previously reported (Huang et al., 2006), so the S249E mutant was made to mimic the modification. EMSA was done on both samples and on an unmodified control to measure affinity for the DBE2 and IRE sequences (Figures 5D and E). DNA affinity for both the Akt phosphorylated FoxO1 and the S249E mutant were found to be unchanged, compared with unmodified FoxO1, confirming that these posttranslational modifications do not affect the DNA-binding activity of FoxO1 under the conditions tested.

DISCUSSION

DNA recognition by members of the 43 human forkhead domain-containing proteins is diverse in terms of sequence recognition and structural mode of binding. The C-terminal wing 2 region of forkhead domains is especially diverse in terms of sequence, structure, and extent of DNA interactions (Clark et al., 1993; Jin et al., 1999; Liu et al., 2002; Stroud et al., 2006; Tsai et al., 2006). Notably, none of the FoxO1/DNA complexes reported here shows ordered electron density for wing 2, suggesting that wing 2 is highly flexible and disordered in the crystal lattice. Further investigation revealed that wing 2 is necessary for high-affinity DNA binding by FoxO1. This observation suggests that wing 2 enhances affinity through forming transient and/or multiple nonspecific electrostatic interactions with the phosphate backbone of the DNA. This hypothesis is supported by the observation that acetylation of Lys245 and Lys248 in wing 2 by CBP/p300 reduces DNA-binding affinity (Figure 5c).

Comparison of the FoxO1/DBE and /IRE DNA structures also reveals new details about how forkhead domains can preferentially bind one sequence over another slightly different sequence. The more favorable interaction of His215 with the carbonyl oxygen of Thy7′ of the DBE DNA sequence likely accounts for most of the 2-fold difference in affinity between the DBE1 and IRE DNA (Figure 5A). The DBE2 DNA, with thymine rich 3′ flanking bases, exhibited a 5-fold increase in FoxO1 DBD affinity over DBE1, suggesting that the 3′ flanking sequence may be a factor for optimal DNA binding by FoxO1. The FoxO1/DBE2 structure reveals that the 3′ flanking region of the DNA is more bent and distorted, compared with the FoxO1/DBE1 structure (Figure 2D). In all three structures reported here, the DNA forms a pseudo-continuous helix in the crystal lattice, so it is possible that crystal packing has influenced the DNA geometry for the structures; however, the difference in affinity combined with the evidence that wing 2 contributes to DNA binding in this region suggests that the increased A-T content in the 3′ flanking region of the DBE2 DNA may allow for more DNA bending and more optimal interaction with wing 2 of FoxO1. It has been reported for FoxA transcription factors that DNA response element affinity can determine the timing of gene expression in embryonic development (Gaudet and Mango, 2002). It would be interesting to investigate whether this holds true for FoxO transcription factors. Genes regulated by high-affinity DBE sequences may have a different timing of expression or level of expression, compared with genes regulated by lower affinity IRE sequences.

Acetylation of the wing 2 region of FoxO by CBP/p300 has been previously shown to alter transcriptional activity of the protein (Brunet et al., 2004; Daitoku et al., 2004; Fukuoka et al., 2003; Jing et al., 2007; Matsuzaki et al., 2005; Motta et al., 2004; Nakae et al., 2003; van der Horst et al., 2004). Our studies show that this change in activity can work, at least in part, via a direct reduction in FoxO1/DNA affinity. However, this decrease in DNA binding by FoxO1 as a function of wing 2 acetylation is not nearly as dramatic as the decrease in DNA binding that is caused by MST1-mediated phosphorylation. In light of this fact, it is possible that CBP/p300-mediated acetylation of FoxO1 may also change the transcriptional activity of FoxO through altering protein-protein interactions that are necessary for FoxO-mediated transcriptional regulation.

Regulation of FoxO1 activity by Akt, CDK1/2, and MST1 kinases is reported to work by three different mechanisms. Akt kinase phosphorylation of Ser256 was found to have no direct effect on DNA binding (Figure 5D). This finding is consistent with regulation through an inhibitory interaction with 14-3-3 proteins

and is also consistent with data showing that wing 2 DNA interactions do not extend to Ser256 (Figure 4). CDK2 phosphorylation of Ser249 was mimicked with a S249E mutant. This mutant was found to have DNA-binding affinity similar to that of unmodified FoxO1 DBD (Figure 5E). This finding is also consistent with the proposed mechanism by which phosphorylation of Ser249 regulates FoxO1 activity indirectly by disrupting the FoxO1 interaction with 14-3-3 proteins or by blocking the adjacent nuclear localization signal (Huang et al., 2006; Yuan et al., 2008). Interestingly, MST1 phosphorylation of Ser212, 218, 234, and 235 was found to almost completely block DNA binding by FoxO1. This finding is consistent with our observation that the target serines are making direct or water-mediated contacts to the phosphate backbone (Figure 2E–G); however, this suggests that the proposed mechanism by which MST1 phosphorylation promotes nuclear translocation and transcription of FoxO1 target genes requires an additional step. We propose that dephosphorylation of serines 212, 218, 234, and 235 occurs before DNA binding and transcriptional regulation by MST1-restored FoxO1. Alternatively, MST1-phosphorylated FoxO1 may participate in transcriptional regulation through association with other regulatory proteins rather than binding DNA directly.

The diverse biological roles of the FoxO family of transcription factors and the mechanisms by which FoxO activity is regulated in the cell remain incompletely understood. Previous reports have indicated that FoxOs are tumor suppressors and mediators of longevity as both downstream targets of insulin signaling and as substrates for Sir2 deacetylase (Biggs et al., 1999; Brunet et al., 1999, 2004; Daitoku et al., 2004; Fukuoka et al., 2003; Kenyon et al., 1993; Motta et al., 2004; Paik et al., 2007; Rena et al., 1999; Tang et al., 1999; van der Horst et al., 2004). The three crystal structures reported herein help to explain the structural basis for DNA recognition by FoxO1 and the factors that contribute to optimal DNA binding by FoxO1. Our rigorous evaluation of DNA-binding affinity of directly acetylated and phosphorylated FoxO1 DBD also provides a more complete understanding of FoxO1 regulation by posttranslational modification, and how misregulation of FoxO may lead to disease.

EXPERIMENTAL PROCEDURES

Protein Expression and Purification

The gene encoding human FoxO1, amino acids 151–266, was cloned into a pETDuet-1 vector containing the gene for yeast SMT3, a ubiquitin-like protein of the SUMO family, in the first multiple cloning site. Overnight expression at 15°C in BL21(DE3)LysS (Novagen) yields a 6× histidine-SUMO-FoxO1 fusion protein. Following lysis and Ni-NTA purification, the His-SUMO tag was removed by incubation with ULP1 (Ubiquitin-like-specific protease 1) at 4°C overnight. The FoxO1 DBD was further purified by cation exchange, ammonium sulfate precipitation, and Superdex-75 size exclusion chromatography in 20 mM HEPES (pH 7.5), 150 mM NaCl, 0.5 mM EDTA, and 2 mM DTT buffer. The protein was finally concentrated to 8 mg/ml and stored at 4°C until use. Protein mutants were generated by site-directed mutagenesis based on the QuickChange protocol from Stratagene (Braman et al., 1996). The FoxO1 DBD truncation constructs and point mutants were purified as described above.

Crystallization

DNA for binding assays and crystallization was purchased from Integrated DNA Technologies (Coralville, IA). The IRE sequence contains strands 5′-CAAGCAAAACAAACCA-3′ and 5′-TGGTTTGTTTTGCTTG-3′. The DBE1 sequence contains strands 5′-CAAGGTAAACAAACCA-3′ and 5′-TGGTTTGTTTACCTTG-3′. The DBE2 sequence contains strands 5′-CAAAATGTAAACAAGA-3′ and 5′-TCTTGTTTACATTTTG-3′. Complementary strands were annealed in 20 mM HEPES (pH 7.5) and 50 mM NaCl buffer by heating to 80°C for 10 min and slowly cooling to room temperature for 3 hr. FoxO1-DNA complexes for crystallization were prepared by mixing concentrated FoxO1 DBD, amino acids 151–266 for the IRE and DBE2 structures and 151–249 for the DBE1 structure, with concentrated, annealed DNA in a 1:1.2 molar ratio. The final concentration of FoxO1 for crystallization was 5 mg/ml. Crystals of FoxO1 DBD/IRE DNA were grown by hanging drop vapor diffusion in 4 days at 4°C using a well solution containing 50 mM sodium cacodylate (pH 6.8), 0.2 M NH_4Cl, 0.01 M $CaCl_2$, and 30% PEG 4,000. Crystals of FoxO1 DBD/DBE1 DNA were grown under the same conditions except with 50 mM HEPES (pH 7.9) and 22% PEG 4,000. Crystals of FoxO1 DBD/DBE2 DNA were also grown under the same conditions except with 50 mM sodium cacodylate (pH 6.4) and 21% PEG 4,000. All crystals were frozen in well solution plus 25% glycerol for cryoprotection. The IRE-containing crystals formed in the space group $P2_12_12$, the DBE1-containing crystals formed in the space group I222, and the DBE2-containing crystals formed in the space group $P3_2$. Soaking in mercury chloride changed cysteine mutant FoxO1 DBD/IRE crystals from the $P2_12_12$ space group to the I222 space group with approximately the same unit cell dimensions.

Data Collection and Structure Determination

Native data sets were collected at the NSLS X6A and APS 23ID-B beamlines. Mercury-soaked FoxO1 S184C and A207C bound to IRE DNA data sets were collected on a Rigaku Raxis-IV home source. Data were processed using HKL2000 (Otwinowski and Minor, 1997). Single Isomorphous Replacement (SIR) was performed with Solve and Resolve (Terwilliger, 2000; Terwilliger and Berendzen, 1999) to find two mercury sites in a FoxO1 DBD S184C mutant/IRE DNA crystal. A mercury-soaked A207C mutant data set was initially set as the native data set, since mercury soaking changed the space group to I222, and the native data set was in the $P2_12_12$ space group. Initial model building with Coot (Emsley and Cowtan, 2004) and refinement with CNS (Brunger et al., 1998) yielded a low-resolution structure that was used for molecular replacement into the higher resolution native $P2_12_12$ (IRE DNA) and $P3_2$ (DBE2 DNA) space groups using Phaser (Read, 2001; Storoni et al., 2004). The DBE1 DNA structure, also in the I222 space group, was solved later using Phaser and the FoxO1 DBD/IRE DNA complex as a search model. Models were initially refined with simulated annealing, energy minimization, and group B-factor refinement. For later stages of refinement, ions and solvent molecules were added to the model, and individual atomic B-factors were refined. The final model was checked for errors against a simulated annealing omit map. Refinement of all three structures resulted in models with excellent statistics and geometries (Table 1). Figures were prepared using PyMOL (DeLano Scientific, Palo Alto, CA).

MST1 Phosphorylation

Human full-length MST1 kinase was amplified and cloned into a pACHis-tev baculoviral transfer vector. Recombinant viruses were selected, amplified, and harvested in Sf9 cells, as described elsewhere (Hutchison et al., 1998). Cells were lysed in 50 mM TRIS (pH 8.0), 400 mM NaCl, 2 mM imidazole, and 1 mM β-mercaptoethanol supplemented with protease inhibitors. The clarified supernatant was loaded onto Ni-NTA agarose, washed, and eluted with 25 mM HEPES (pH 7.5), 100 mM NaCl, and 200 mM imidazole. The eluted protein was further purified by Superdex-200 size exclusion chromatography in 25 mM HEPES (pH 7.5) and 100 mM NaCl. The eluted fractions were pooled, concentrated to 2 mg/ml, and flash frozen until use. MST1 was incubated with the FoxO1 DBD (151–266) in a 1:10 ratio (MST/FoxO1) at 30°C for 4 hr in buffer containing 20 mM TRIS (pH 7.5), 5 mM $MgCl_2$, and 2 mM ATP. A control sample was also incubated at 30°C for 4 hr in the absence of MST1 or ATP. After 4 hr, the sample was put on ice for 10 min and then injected onto a Superdex-75 size exclusion column to purify the FoxO1 DBD from the MST1 and the ATP. Purified FoxO1 was then concentrated and analyzed by MALDI-TOF mass spectrometry to confirm phosphorylation. The mass of the largest peak corresponded to the addition of four phosphates. Species corresponding to three and five phosphates were also observed (Figure S3A).

p300 Acetylation

p300 (a gift from Xin Liu, Ling Wang, Philip Cole, and R.M.) was incubated with the FoxO1 DBD (151–266) in a 1:20 ratio (p300/FoxO1) at 30°C for 3 hr in buffer

containing 50 mM HEPES (pH 7.5), 0.1 mM EDTA, 1 mM DTT, 0.05 mg/mL BSA, and 3 mM Acetyl-CoA. A control sample was also incubated at 30°C for 3 hr with the same buffer conditions but with p300 absent. After 3 hr, the sample was put on ice for 10 min and then injected onto a Superdex-75 size exclusion column to purify the FoxO1 DBD from the p300 and the Acetyl CoA. Purified FoxO1 was then concentrated and analyzed by MALDI-TOF mass spectrometry to confirm acetylation. Results indicated one distinct species with an increased mass of 172 Da or approximately four acetyl groups (Figure S4A). A combination of papain digestion, MALDI-TOF mass spectrometry, and N-terminal sequencing was used to confirm that the acetyl groups were added to the C terminus of FoxO1 (amino acids 245–266) (Figures S2B and S4C).

Akt Phosphorylation

Akt1 (PKB α) was purchased (Biomol International, SE-416) and incubated with the FoxO1 DBD (151–266) at 30°C for 3 hr in buffer containing 25 mM MOPS (pH 7.2), 12.5 mM β-glycerophosphate, 25 mM $MgCl_2$, 5 mM EGTA, 2 mM EDTA, 0.4 mM DTT, and 2 mM ATP. A control sample was also incubated at 30°C for 3 hr with the same buffer conditions but with Akt absent. After 3 hr, the sample was put on ice for 10 min and then injected onto a Superdex-75 size exclusion column to purify the FoxO1 DBD from the Akt and the ATP. Purified FoxO1 was then concentrated and analyzed by MALDI-TOF mass spectrometry to confirm phosphorylation. Results showed one distinct species with an increased mass of 90 Da or approximately one phosphate group (Figure S5A).

DNA-Binding Assays

EMSAs were done with biotinylated DNA duplexes (Integrated DNA Technologies, Coralville, IA) and developed with a chemiluminescent nucleic acid detection kit (Pierce 89880). Briefly, a serial dilution of FoxO1 protein was prepared to give a final concentration range of 1 μM to 0.5 nM FoxO1. FoxO1 serial dilutions were each equilibrated at room temperature with 1 nM DNA for 30 min in binding buffer containing 20 mM TRIS (pH 8.0), 50 mM KCl, 5% glycerol, 2 mM DTT, 0.2 mM EDTA, 2 mM $MgCl_2$, 0.1 mg/mL BSA, and 1 ng/uL poly dI·dC. The equilibrated mixture was loaded onto a 6% DNA retardation gel (Invitrogen) in 0.5× TRIS-borate-EDTA (TBE) and run at 100 V for 1 hr at 4°C. The gel was blotted onto a Biodyne B (Invitrogen) membrane at 380 mA for 1 hr in 0.5× TBE at 4°C. The blotted DNA was cross-linked to the membrane using a Stratagene cross-linker. The membrane was developed according to the nucleic acid detection protocol from Pierce. Films were then exposed, developed, and scanned. All assays were done in duplicate. Apparent K_d values were determined by measuring shifted band intensity with ImageJ (from the NIH; http://rsb.info.nih.gov/ij/) and fitting a plot of intensity versus Log[FoxO1] to one-site competitive binding in GraphPad Prism software.

ACCESSION NUMBERS

Coordinates for the FoxO1 DBD/IRE, /DBE1, and /DBE2 DNA complexes have been deposited in the Protein Data Bank with accession codes 3COA, 3CO6, and 3CO7, respectively.

SUPPLEMENTAL DATA

Supplemental data include five figures and can be found with this article online at http://www.structure.org/cgi/content/full/16/9/1407/DC1/.

ACKNOWLEDGMENTS

We would like to thank Mary Fitzgerald, Manqing Hong, Santosh Hodawadekar, Troy Messick, Brandi Sanders, and other members of the Marmorstein Laboratory for helpful discussions. We thank Xin Liu, Ling Wang, and Philip Cole for the contribution of purified p300. We also thank Nicole DiFlorio and Matt Hart of Wistar Proteomics, and Marc Allaire, Fabiano Yokaichiya and Jean Jakoncic of NSLS beamline X6A for help with data collection. This work was supported by an NIH grant to R.M. (GM 052880).

Received: January 29, 2008
Revised: April 9, 2008
Accepted: June 9, 2008
Published: September 9, 2008

REFERENCES

Anderson, M.J., Viars, C.S., Czekay, S., Cavenee, W.K., and Arden, K.C. (1998). Cloning and characterization of three human forkhead genes that comprise an FKHR-like gene subfamily. Genomics *47*, 187–199.

Biggs, W.H., 3rd, Meisenhelder, J., Hunter, T., Cavenee, W.K., and Arden, K.C. (1999). Protein kinase B/Akt-mediated phosphorylation promotes nuclear exclusion of the winged helix transcription factor FKHR1. Proc. Natl. Acad. Sci. USA *96*, 7421–7426.

Borkhardt, A., Repp, R., Haas, O.A., Leis, T., Harbott, J., Kreuder, J., Hammermann, J., Henn, T., and Lampert, F. (1997). Cloning and characterization of AFX, the gene that fuses to MLL in acute leukemias with a t(X;11)(q13;q23). Oncogene *14*, 195–202.

Boura, E., Silhan, J., Herman, P., Vecer, J., Sulc, M., Teisinger, J., Obsilova, V., and Obsil, T. (2007). Both the N-terminal loop and wing W2 of the forkhead domain of transcription factor Foxo4 are important for DNA binding. J. Biol. Chem. *282*, 8265–8275.

Braman, J., Papworth, C., and Greener, A. (1996). Site-directed mutagenesis using double-stranded plasmid DNA templates. Methods Mol. Biol. *57*, 31–44.

Brunet, A., Bonni, A., Zigmond, M.J., Lin, M.Z., Juo, P., Hu, L.S., Anderson, M.J., Arden, K.C., Blenis, J., and Greenberg, M.E. (1999). Akt promotes cell survival by phosphorylating and inhibiting a forkhead transcription factor. Cell *96*, 857–868.

Brunet, A., Sweeney, L.B., Sturgill, J.F., Chua, K.F., Greer, P.L., Lin, Y., Tran, H., Ross, S.E., Mostoslavsky, R., Cohen, H.Y., et al. (2004). Stress-dependent regulation of FOXO transcription factors by the SIRT1 deacetylase. Science *303*, 2011–2015.

Brunger, A.T., Adams, P.D., Clore, G.M., DeLano, W.L., Gros, P., Grosse-Kunstleve, R.W., Jiang, J.S., Kuszewski, J., Nilges, M., Pannu, N.S., et al. (1998). Crystallography & NMR system: a new software suite for macromolecular structure determination. Acta Crystallogr. D Biol. Crystallogr. *54*, 905–921.

Cheong, J.W., Eom, J.I., Maeng, H.Y., Lee, S.T., Hahn, J.S., Ko, Y.W., and Min, Y.H. (2003). Constitutive phosphorylation of FKHR transcription factor as a prognostic variable in acute myeloid leukemia. Leuk. Res. *27*, 1159–1162.

Clark, K.L., Halay, E.D., Lai, E., and Burley, S.K. (1993). Co-crystal structure of the HNF-3/fork head DNA-recognition motif resembles histone H5. Nature *364*, 412–420.

Daitoku, H., Hatta, M., Matsuzaki, H., Aratani, S., Ohshima, T., Miyagishi, M., Nakajima, T., and Fukamizu, A. (2004). Silent information regulator 2 potentiates Foxo1-mediated transcription through its deacetylase activity. Proc. Natl. Acad. Sci. USA *101*, 10042–10047.

Davis, R.J., D'Cruz, C.M., Lovell, M.A., Biegel, J.A., and Barr, F.G. (1994). Fusion of PAX7 to FKHR by the variant t(1;13)(p36;q14) translocation in alveolar rhabdomyosarcoma. Cancer Res. *54*, 2869–2872.

Emsley, P., and Cowtan, K. (2004). Coot: model-building tools for molecular graphics. Acta Crystallogr. D Biol. Crystallogr. *60*, 2126–2132.

Fukuoka, M., Daitoku, H., Hatta, M., Matsuzaki, H., Umemura, S., and Fukamizu, A. (2003). Negative regulation of forkhead transcription factor AFX (Foxo4) by CBP-induced acetylation. Int. J. Mol. Med. *12*, 503–508.

Furuyama, T., Nakazawa, T., Nakano, I., and Mori, N. (2000). Identification of the differential distribution patterns of mRNAs and consensus binding sequences for mouse DAF-16 homologues. Biochem. J. *349*, 629–634.

Galili, N., Davis, R.J., Fredericks, W.J., Mukhopadhyay, S., Rauscher, F.J., 3rd, Emanuel, B.S., Rovera, G., and Barr, F.G. (1993). Fusion of a fork head domain gene to PAX3 in the solid tumour alveolar rhabdomyosarcoma. Nat. Genet. *5*, 230–235.

Gaudet, J., and Mango, S.E. (2002). Regulation of organogenesis by the *Caenorhabditis elegans* FoxA protein PHA-4. Science *295*, 821–825.

Gottlieb, S., and Ruvkun, G. (1994). daf-2, daf-16 and daf-23: genetically interacting genes controlling Dauer formation in *Caenorhabditis elegans*. Genetics *137*, 107–120.

Greer, E.L., and Brunet, A. (2005). FOXO transcription factors at the interface between longevity and tumor suppression. Oncogene *24*, 7410–7425.

Guo, S., Rena, G., Cichy, S., He, X., Cohen, P., and Unterman, T. (1999). Phosphorylation of serine 256 by protein kinase B disrupts transactivation by FKHR and mediates effects of insulin on insulin-like growth factor-binding protein-1 promoter activity through a conserved insulin response sequence. J. Biol. Chem. *274*, 17184–17192.

Hillion, J., Le Coniat, M., Jonveaux, P., Berger, R., and Bernard, O.A. (1997). AF6q21, a novel partner of the MLL gene in t(6;11)(q21;q23), defines a forkhead transcriptional factor subfamily. Blood *90*, 3714–3719.

Hu, M.C., Lee, D.F., Xia, W., Golfman, L.S., Ou-Yang, F., Yang, J.Y., Zou, Y., Bao, S., Hanada, N., Saso, H., et al. (2004). IkappaB kinase promotes tumorigenesis through inhibition of forkhead FOXO3a. Cell *117*, 225–237.

Huang, H., and Tindall, D.J. (2007). Dynamic FoxO transcription factors. J. Cell Sci. *120*, 2479–2487.

Huang, H., Regan, K.M., Lou, Z., Chen, J., and Tindall, D.J. (2006). CDK2-dependent phosphorylation of FOXO1 as an apoptotic response to DNA damage. Science *314*, 294–297.

Hutchison, M., Berman, K.S., and Cobb, M.H. (1998). Isolation of TAO1, a protein kinase that activates MEKs in stress-activated protein kinase cascades. J. Biol. Chem. *273*, 28625–28632.

Jin, C., Marsden, I., Chen, X., and Liao, X. (1999). Dynamic DNA contacts observed in the NMR structure of winged helix protein-DNA complex. J. Mol. Biol. *289*, 683–690.

Jing, E., Gesta, S., and Kahn, C.R. (2007). SIRT2 regulates adipocyte differentiation through FoxO1 acetylation/deacetylation. Cell Metab. *6*, 105–114.

Kaestner, K.H., Knochel, W., and Martinez, D.E. (2000). Unified nomenclature for the winged helix/forkhead transcription factors. Genes Dev. *14*, 142–146.

Kenyon, C., Chang, J., Gensch, E., Rudner, A., and Tabtiang, R. (1993). A *C. elegans* mutant that lives twice as long as wild type. Nature *366*, 461–464.

Kops, G.J., de Ruiter, N.D., De Vries-Smits, A.M., Powell, D.R., Bos, J.L., and Burgering, B.M. (1999). Direct control of the forkhead transcription factor AFX by protein kinase B. Nature *398*, 630–634.

Larsen, P.L., Albert, P.S., and Riddle, D.L. (1995). Genes that regulate both development and longevity in *Caenorhabditis elegans*. Genetics *139*, 1567–1583.

Lehtinen, M.K., Yuan, Z., Boag, P.R., Yang, Y., Villen, J., Becker, E.B., DiBacco, S., de la Iglesia, N., Gygi, S., Blackwell, T.K., and Bonni, A. (2006). A conserved MST-FOXO signaling pathway mediates oxidative-stress responses and extends life span. Cell *125*, 987–1001.

Liu, P.P., Chen, Y.C., Li, C., Hsieh, Y.H., Chen, S.W., Chen, S.H., Jeng, W.Y., and Chuang, W.J. (2002). Solution structure of the DNA-binding domain of interleukin enhancer binding factor 1 (FOXK1a). Proteins *49*, 543–553.

Matsuzaki, H., Daitoku, H., Hatta, M., Aoyama, H., Yoshimochi, K., and Fukamizu, A. (2005). Acetylation of Foxo1 alters its DNA-binding ability and sensitivity to phosphorylation. Proc. Natl. Acad. Sci. USA *102*, 11278–11283.

Mazet, F., Yu, J.K., Liberles, D.A., Holland, L.Z., and Shimeld, S.M. (2003). Phylogenetic relationships of the Fox (Forkhead) gene family in the Bilateria. Gene *316*, 79–89.

Modur, V., Nagarajan, R., Evers, B.M., and Milbrandt, J. (2002). FOXO proteins regulate tumor necrosis factor-related apoptosis inducing ligand expression. Implications for PTEN mutation in prostate cancer. J. Biol. Chem. *277*, 47928–47937.

Motta, M.C., Divecha, N., Lemieux, M., Kamel, C., Chen, D., Gu, W., Bultsma, Y., McBurney, M., and Guarente, L. (2004). Mammalian SIRT1 represses forkhead transcription factors. Cell *116*, 551–563.

Myatt, S.S., and Lam, E.W. (2007). The emerging roles of forkhead box (Fox) proteins in cancer. Nat. Rev. Cancer *7*, 847–859.

Nakae, J., Kitamura, T., Kitamura, Y., Biggs, W.H., 3rd, Arden, K.C., and Accili, D. (2003). The forkhead transcription factor Foxo1 regulates adipocyte differentiation. Dev. Cell *4*, 119–129.

Ogg, S., Paradis, S., Gottlieb, S., Patterson, G.I., Lee, L., Tissenbaum, H.A., and Ruvkun, G. (1997). The forkhead transcription factor DAF-16 transduces insulin-like metabolic and longevity signals in C. elegans. Nature *389*, 994–999.

Otwinowski, Z., and Minor, W. (1997). Processing of X-ray diffraction data collected in oscillation mode. Methods Enzymol. *276*, 307–326.

Paik, J.H., Kollipara, R., Chu, G., Ji, H., Xiao, Y., Ding, Z., Miao, L., Tothova, Z., Horner, J.W., Carrasco, D.R., et al. (2007). FoxOs are lineage-restricted redundant tumor suppressors and regulate endothelial cell homeostasis. Cell *128*, 309–323.

Parry, P., Wei, Y., and Evans, G. (1994). Cloning and characterization of the t(X;11) breakpoint from a leukemic cell line identify a new member of the forkhead gene family. Genes Chromosomes Cancer *11*, 79–84.

Read, R.J. (2001). Pushing the boundaries of molecular replacement with maximum likelihood. Acta Crystallogr. D Biol. Crystallogr. *57*, 1373–1382.

Rena, G., Guo, S., Cichy, S.C., Unterman, T.G., and Cohen, P. (1999). Phosphorylation of the transcription factor forkhead family member FKHR by protein kinase B. J. Biol. Chem. *274*, 17179–17183.

Seoane, J., Le, H.V., Shen, L., Anderson, S.A., and Massague, J. (2004). Integration of Smad and forkhead pathways in the control of neuroepithelial and glioblastoma cell proliferation. Cell *117*, 211–223.

Storoni, L.C., McCoy, A.J., and Read, R.J. (2004). Likelihood-enhanced fast rotation functions. Acta Crystallogr. D Biol. Crystallogr. *60*, 432–438.

Stroud, J.C., Wu, Y., Bates, D.L., Han, A., Nowick, K., Paabo, S., Tong, H., and Chen, L. (2006). Structure of the forkhead domain of FOXP2 bound to DNA. Structure *14*, 159–166.

Sunters, A., Madureira, P.A., Pomeranz, K.M., Aubert, M., Brosens, J.J., Cook, S.J., Burgering, B.M., Coombes, R.C., and Lam, E.W. (2006). Paclitaxel-induced nuclear translocation of FOXO3a in breast cancer cells is mediated by c-Jun NH2-terminal kinase and Akt. Cancer Res. *66*, 212–220.

Tang, E.D., Nunez, G., Barr, F.G., and Guan, K.L. (1999). Negative regulation of the forkhead transcription factor FKHR by Akt. J. Biol. Chem. *274*, 16741–16746.

Terwilliger, T.C. (2000). Maximum-likelihood density modification. Acta Crystallogr. D Biol. Crystallogr. *56*, 965–972.

Terwilliger, T.C., and Berendzen, J. (1999). Automated MAD and MIR structure solution. Acta Crystallogr. D Biol. Crystallogr. *55*, 849–861.

Tissenbaum, H.A., and Guarente, L. (2001). Increased dosage of a sir-2 gene extends lifespan in *Caenorhabditis elegans*. Nature *410*, 227–230.

Tsai, K.L., Huang, C.Y., Chang, C.H., Sun, Y.J., Chuang, W.J., and Hsiao, C.D. (2006). Crystal structure of the human FOXK1a-DNA complex and its implications on the diverse binding specificity of winged helix/forkhead proteins. J. Biol. Chem. *281*, 17400–17409.

van der Horst, A., Tertoolen, L.G., de Vries-Smits, L.M., Frye, R.A., Medema, R.H., and Burgering, B.M. (2004). FOXO4 is acetylated upon peroxide stress and deacetylated by the longevity protein hSir2(SIRT1). J. Biol. Chem. *279*, 28873–28879.

van Dongen, M.J., Cederberg, A., Carlsson, P., Enerback, S., and Wikstrom, M. (2000). Solution structure and dynamics of the DNA-binding domain of the adipocyte-transcription factor FREAC-11. J. Mol. Biol. *296*, 351–359.

Weigelt, J., Climent, I., Dahlman-Wright, K., and Wikstrom, M. (2001). Solution structure of the DNA binding domain of the human forkhead transcription factor AFX (FOXO4). Biochemistry *40*, 5861–5869.

Yuan, Z., Becker, E.B., Merlo, P., Yamada, T., DiBacco, S., Konishi, Y., Schaefer, E.M., and Bonni, A. (2008). Activation of FOXO1 by Cdk1 in cycling cells and postmitotic neurons. Science *319*, 1665–1668.

